

# Tyr130 phosphorylation triggers Syk release from antigen receptor by long-distance conformational uncoupling

Yajie Zhang<sup>\*†</sup>, Hyunju Oh<sup>\*</sup>, Robert A. Burton<sup>\*‡</sup>, John W. Burgner<sup>§¶</sup>, Robert L. Geahlen<sup>\*||</sup>, and Carol Beth Post<sup>\*§||\*\*</sup>

<sup>\*</sup>Department of Medicinal Chemistry and Molecular Pharmacology, <sup>§</sup>Markey Center for Structural Biology, <sup>¶</sup>Bindley Bioscience Center and <sup>||</sup>Purdue Cancer Center, Purdue University, West Lafayette, IN 47907

Edited by Adriaan Bax, National Institutes of Health, Bethesda, MD, and approved May 29, 2008 (received for review September 10, 2007)

The Syk protein-tyrosine kinase plays a major role in signaling through the B cell receptor for antigen (BCR). Syk binds the receptor via its tandem pair of SH2 domains interacting with a doubly phosphorylated immunoreceptor tyrosine-based activation motif (dp-ITAM) of the BCR complex. Upon phosphorylation of Tyr-130, which lies between the two SH2 domains distant to the phosphotyrosine binding sites, Syk dissociates from the receptor. To understand the structural basis for this dissociation, we investigated the structural and dynamic characteristics of the wild type tandem SH2 region (tSH2) and a variant tandem SH2 region (tSH2<sub>pm</sub>) with Tyr-130 substituted by Glu to permanently introduce a negative charge at this position. NMR heteronuclear relaxation experiments, residual dipolar coupling measurements and analytical ultracentrifugation revealed substantial differences in the hydrodynamic behavior of tSH2 and tSH2<sub>pm</sub>. Although the two SH2 domains in tSH2 are tightly associated, the two domains in tSH2<sub>pm</sub> are partly uncoupled and tumble in solution with a faster correlation time. In addition, the equilibrium dissociation constant for the binding of tSH2<sub>pm</sub> to dp-ITAM (1.8  $\mu$ M) is significantly higher than that for the interaction between dp-ITAM and tSH2 but is close to that for a singly tyrosine-phosphorylated peptide binding to a single SH2 domain. Experimental data and hydrodynamic calculations both suggest a loss of domain-domain contacts and change in relative orientation upon the introduction of a negative charge on residue 130. A long-distance structural mechanism by which the phosphorylation of Y130 negatively regulates the interaction of Syk with immune receptors is proposed.

allosteric regulation | multidomain dynamics | Syk kinase regulation | tyrosine phosphorylation | NMR <sup>15</sup>N relaxation

Syk, a 72-kDa cytoplasmic protein-tyrosine kinase essential to receptor-mediated signaling in B cells, has two N-terminal SH2 domains connected by a 45-residue region (interdomain A). These tandem SH2 domains are separated by a longer, 104-residue region (interdomain B) from a C-terminal kinase domain. Syk mediates B cell signaling through a variety of immune-recognition receptors, including the B cell antigen receptor (BCR). The receptors have similar subunits bearing cytoplasmic, immunoreceptor tyrosine-based activation motifs (ITAMs) (1) with the consensus sequence YXX(L/I)-X<sub>6-9</sub>-YXX(L/I) (2). Phosphorylation on both ITAM tyrosine residues occurs after receptor engagement and is required for Syk binding via the tandem SH2 domains to initiate subsequent signaling cascades (3). Zap-70, the other member of the Syk family, functions similarly in T cell receptor signaling as Syk does in B cells. Events of receptor-dependent signaling in these two cells are highly analogous.

Syk is physically and functionally coupled to receptors with ITAMs that vary in the sequence and length of the spacer that separates the two phosphotyrosines (4). The tandem SH2 domains associate with high affinity in a head-to-tail orientation with each SH2 domain binding to one of the two phosphotyrosines of ITAM. Arginine residues 22 and 42 of N-SH2 and 175 and 195 of C-SH2 directly contribute to the network of hydrogen bonds coordinating

the phosphate groups. Structural and biophysical studies indicate that the adaptability of the Syk tandem SH2 domains is made possible by relatively weak interactions between the two SH2 domains and the flexibility of interdomain A (5–8).

In stimulated cells, the interaction of Syk with the phosphorylated ITAM of clustered antigen receptors leads to phosphorylation of Syk itself on multiple tyrosines through a combination of autophosphorylation and phosphorylation *in trans* by Src-family tyrosine kinases (9, 10). These phosphorylations both modulate Syk's catalytic activity (11) and generate docking sites for SH2 domain-containing proteins, such as c-Cbl, PLC $\gamma$ , and Vav1. Alternative patterns of phosphorylation in interdomain B are differentially recognized, such as the preferential binding of a doubly phosphorylated region by a single SH2 of PLC $\gamma$  (12), and elicit either inhibitory or activating effects on downstream signaling events according to the binding partner (13, 14).

Despite the tight binding of tandem SH2 domains to phosphorylated ITAM, much of the activated, tyrosine-phosphorylated Syk can be found dissociated from the receptor (15). Syk has even been identified in the nucleus of activated lymphocytes (16, 17). One factor that has been proposed for modulating the interactions of Syk with the receptor ITAM is the phosphorylation of Syk on Y130 (11), even though Y130 is >20 Å away from either of the two SH2 binding sites. The covalent modification of Y130 occurs readily *in vitro* through autophosphorylation and has been observed in cells treated with protein-tyrosine phosphatase inhibitors (18). Once phosphorylated, Syk is not found associated with the activated B cell antigen receptor (BCR) complex, an effect that can be mimicked by replacing Y130 with a glutamate (11). In cells expressing a Syk(Y130E) variant, the variant exhibits a greatly reduced ability to associate with the clustered BCR, and BCR-dependent phosphorylation of cellular proteins is dampened. Kinase-receptor interactions and receptor-stimulated protein-tyrosine phosphorylation are, however, enhanced in cells expressing Syk(Y130F), which cannot be phosphorylated within interdomain A. Thus, the acquisition of a negatively charged residue within interdomain A diminishes association of Syk with the antigen receptor. The structural basis for this effect was unknown.

We have investigated the molecular mechanism for how the acquisition of negative charge at the remote position Y130 regulates

Author contributions: Y.Z., R.A.B., J.W.B., R.L.G., and C.B.P. designed research; Y.Z., H.O., and J.W.B. performed research; Y.Z., J.W.B., R.L.G., and C.B.P. analyzed data; and Y.Z., R.L.G., and C.B.P. wrote the paper.

The authors declare no conflict of interest.

This article is a PNAS Direct Submission.

<sup>†</sup>Present address: Harvard Medical School, Boston, MA 02115.

<sup>‡</sup>Present address: BAE Systems, Advanced Technologies, 1250 North 24th Street, Washington, DC 20037.

<sup>\*\*</sup>To whom correspondence should be addressed. E-mail: cbp@purdue.edu.

This article contains supporting information online at [www.pnas.org/cgi/content/full/0708583105/DCSupplemental](http://www.pnas.org/cgi/content/full/0708583105/DCSupplemental).

© 2008 by The National Academy of Sciences of the USA

against the association of Syk with antigen receptor. First, we present evidence that modulation of receptor association by Y130 phosphorylation is the result of diminished affinity (20- to 1,000-fold) of Syk for the ITAM, and that Y130 is phosphorylated in stimulated cells. How the acquisition of negative charge at position 130 alters the structural and dynamic properties of the tandem SH2 region of Syk is elucidated by NMR studies, coupled with analytical ultracentrifugation and theoretical hydrodynamic calculations conducted on a 28-kDa Syk construct comprising the two SH2 domains plus interdomain A (tSH2) and on the same construct with the substitution Y130E to mimic phosphorylation (tSH2<sub>pm</sub>). Glutamic acid substitution of tyrosine is commonly used for experiments in cells to mimic Tyr phosphorylation, and the results are generally accepted to report on the functional mechanisms of phosphorylation. The in-cell results described above and the observation from the crystal structure that Y130 has few intramolecular interactions establish the use of Y130E substitution to investigate the structural response to the introduction of negative charge in interdomain A, although we recognize the substitution may not fully reproduce the effects of phosphorylation. We find that negative charge at position 130 disrupts interdomain A structure and SH2-SH2 contact, alters the orientation of the SH2 domains relative to each other, and induces a more extended shape. We propose a model for the long-distance mechanism of the Y130 phosphorylation-dependent dissociation of Syk from immune receptors and discuss its implications in Syk signaling through BCR.

## Results and Discussion

**Tyr-130 Phosphorylation Affects Syk Association with ITAM.** Measurements in cells indicate the interaction of Syk with the BCR is modulated by phosphorylation on Y130 (11). To further define the effect of Y130 phosphorylation on Syk binding to BCR, Syk association was measured in a pull-down assay, using a biotinylated phosphopeptide corresponding in sequence to the doubly phosphorylated ITAM (dp-ITAM) of CD79a immobilized on streptavidin-agarose. Syk was recovered from detergent cell lysates by immobilized dp-ITAM peptide (Fig. 1A, WT) and not by nonphosphorylated ITAM peptide (data not shown). Pretreatment of cells with the phosphatase inhibitor H<sub>2</sub>O<sub>2</sub>, to increase the cellular levels of phosphorylation, reduced by nearly 90% the amount of WT Syk recovered by the immobilized phosphopeptide. Phosphorylation of Syk on Y130 in H<sub>2</sub>O<sub>2</sub>-treated cells was established by phosphopeptide mapping of the protein recovered by immunoprecipitation from cells prelabeled with orthophosphate (Fig. 1B Upper). When Phe is substituted for Y130, the reduction caused by the treatment of cells with H<sub>2</sub>O<sub>2</sub> in the amount of Syk recovered with the dp-ITAM peptide was largely eliminated (Fig. 1A, Y130F); the amount was reduced by only 11%.

The substitution of Y130 with a glutamate residue, Syk(Y130E), mimicking Syk fully phosphorylated at residue 130, eliminated all detectable recovery of Syk to the dp-ITAM peptide (Fig. 1A, Y130E). Furthermore, a catalytically inactive form of Syk [Syk(K396R)], which cannot catalyze the autophosphorylation reaction of Y130, is recovered, and no reduction in response to H<sub>2</sub>O<sub>2</sub> was observed (Fig. 1A, KD). These results indicate that the autophosphorylation of Y130 decreases the binding of Syk to doubly phosphorylated ITAM and the observed (11) reduction in Syk associated with antigen receptor was most likely, therefore, a consequence of the reduced binding of Syk to phosphorylated ITAM tyrosines on BCR components. The pattern of recovered Syk in Fig. 1A for the variants Syk(Y130E) and Syk(Y130F) is similar to that generated by WT in the presence of H<sub>2</sub>O<sub>2</sub> and by KD Syk, respectively. Accordingly, substitution of Y130 is a reasonable mimic for the phosphorylated (Y130E) and unphosphorylated (Y130F) forms of Syk.

Phosphorylation on Y130 in cells was demonstrated only in the presence of the phosphatase inhibitors pervanadate or H<sub>2</sub>O<sub>2</sub> (19). To better characterize Tyr-130 phosphorylation in cells, DT40 cells

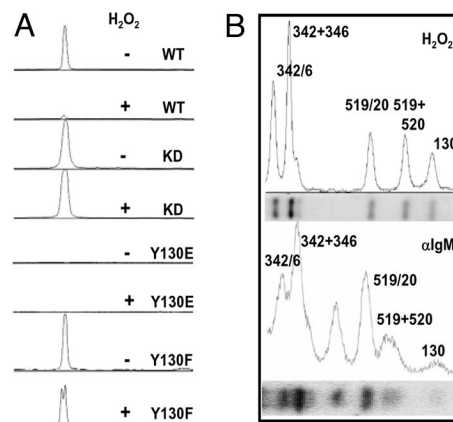


**Fig. 1.** The binding of Syk to a phosphorylated ITAM is inhibited by the autophosphorylation of Y130. (A) Syk-deficient DT40 cells stably expressing Myc-tagged murine Syk (WT), Syk(K396R) (KD), Syk(Y130E) or Syk(Y130F) were treated without (–) or with (+) the phosphatase inhibitor H<sub>2</sub>O<sub>2</sub> (10 mM). Detergent lysates were adsorbed to an immobilized phosphopeptide corresponding to the doubly phosphorylated CD79a ITAM. Bound Syk, plotted here, was detected by Western blot analysis with an anti-Syk antibody and quantified by densitometry. (B) Myc-tagged Syk was immunoprecipitated and anti-Myc antibodies from lysates of cells preincubated in [<sup>32</sup>P]orthophosphate and treated with H<sub>2</sub>O<sub>2</sub> (Upper) or anti-IgM antibodies (Lower). The recovered protein was digested with trypsin and the resulting phosphopeptides separated electrophoretically and detected by autoradiography (Upper) or with a phosphoimager (Lower). The region of the gel containing the smaller and more rapidly migrating phosphopeptides is illustrated. The positions of the phosphotyrosines within each peptide are numbered based on the murine Syk sequence.

expressing Myc-tagged murine Syk were preincubated with [<sup>32</sup>P]orthophosphate and stimulated with anti-IgM antibodies without addition of phosphatase inhibitors. For comparison, results were also obtained for cells treated with the phosphatase inhibitor H<sub>2</sub>O<sub>2</sub>. Syk was immunoprecipitated and digested with trypsin. The resulting phosphorylated peptides (Fig. 1B) demonstrate that Tyr-130 is phosphorylated in anti-IgM-antibody stimulated cells (Lower) and in cells treated with H<sub>2</sub>O<sub>2</sub> (Upper).

The effect of Y130 phosphorylation on the interaction of Syk tSH2 with dp-ITAM peptide was further characterized by sedimentation velocity ultracentrifugation. Binding equilibrium of dp-ITAM with either tSH2 or tSH2<sub>pm</sub> was monitored by direct measure of the fraction of bound peptide as a function of total peptide concentration. The equilibrium dissociation constant estimated for tSH2<sub>pm</sub> is  $1.8 \pm 0.3 \mu\text{M}$  [see supporting information (SI)]. In the case of tSH2, at the lowest detectable concentration, dp-ITAM peptide was fully bound at all concentrations <1:1 molar ratio.  $K_D$  for tSH2 binding dp-ITAM is therefore too low for determination by AUC, a result consistent with reported  $K_D$  values, which range from 2 to 100 nM (5, 6). Given these literature values, tSH2<sub>pm</sub> binds dp-ITAM with 20–1000 times lower affinity than unphosphorylated tSH2. The  $K_D$  value reported here for tSH2<sub>pm</sub> ( $1.8 \mu\text{M}$ ) is similar to that reported for an R45 variant of Syk tSH2 ( $1.3 \mu\text{M}$ ), which interacts with phosphotyrosine only through the C-SH2 domain (20), and to the dissociation constants for single SH2 domains binding to phosphotyrosine peptides ( $1\text{--}10 \mu\text{M}$ ). Introduction of the negative charge at position 130 of tSH2 therefore appears to change the recognition between tSH2 and BCR-ITAM from a high-affinity two-site interaction to a low-affinity single-site interaction.

**Chemical Shift Differences Indicate Structural Changes in Interdomain A and the SH2-SH2 Interface.** A comparison of the <sup>1</sup>H-<sup>15</sup>N HSQC spectra of tSH2 and tSH2<sub>pm</sub> is shown in Fig. 2A. Of the 245 amide cross peaks anticipated from the protein sequence, only 160 peaks were observed for tSH2 and 154 peaks were assigned. Similar

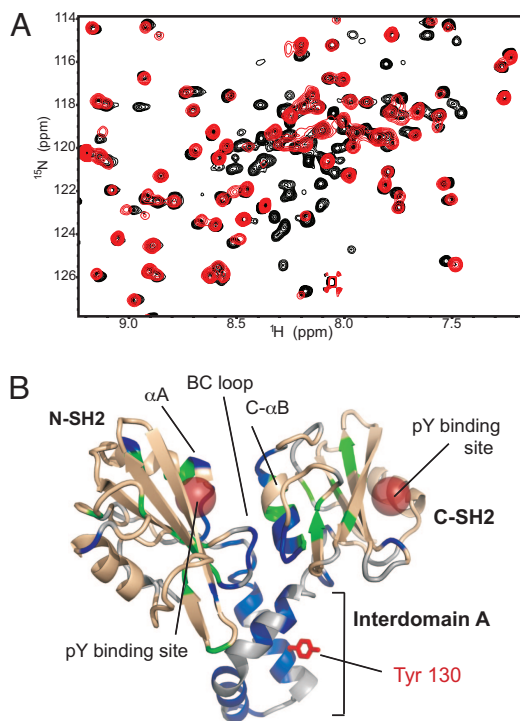


**Fig. 2.** Spectral differences between tSH2 and tSH2<sub>pm</sub>. (A) Overlay of part of the <sup>1</sup>H-<sup>15</sup>N HSQC spectra of tSH2 (red) and tSH2<sub>pm</sub> (black) recorded at 600 MHz, 20°C. A number of peaks from residues in interdomain A and at the SH2 domain interface are observed in the tSH2<sub>pm</sub> spectrum, but missing in the tSH2 spectrum. (B) Spectral differences are mapped onto the crystal structure for the Syk tSH2 complexed with the phosphorylated CD3 $\epsilon$ -ITAM (PDB 1A81). Residues are colored based on HSQC peaks: observed for tSH2 but not tSH2<sub>pm</sub> (blue), a difference in chemical shift >0.04 ppm (green), or <0.04 ppm (tan), not observed (gray). Y130 is shown in sticks. Spheres show the location of the two phosphotyrosine binding pockets. The amide group chemical shift difference between the two protein constructs,  $\Delta_{1H+15N}$ , is calculated from the frequency difference,  $\delta_i$ , of nucleus *i* (33):  $\Delta_{1H+15N} = \sqrt{(\delta_H)^2 + (0.154\delta_N)^2}$ .

results were reported for uncomplexed ZAP-70 tSH2; only 134 of 242 mainchain amide groups were assigned (8). A considerably larger number of resonances (209) are observed for the tSH2<sub>pm</sub>, and 200 were assigned. This set includes all of the resonances assigned for tSH2.

The majority of the chemical shifts for residues in the SH2 domains are nearly identical for tSH2 and tSH2<sub>pm</sub>, indicating that the overall SH2 domain structures are unchanged. A number of residues, however, exhibit larger differences. Residues with chemical shift differences  $\Delta_{1H+15N} > 0.04$  ppm are mapped onto the crystal structure of Syk tSH2 (PDB entry 1A81) in green (Fig. 2B), and resonances missing in the tSH2 HSQC spectrum, but present in the tSH2<sub>pm</sub> spectrum, are in blue. For both comparisons, the majority of the mapped residues are located either in interdomain A or at the interface of the two SH2 domains. Notably, for tSH2, none of the residues in interdomain A have detectable NMR signals, similar to observations for ZAP-70 tSH2 (6–8). Such exchange broadening of resonances indicates this linker region interconverts between conformations on a  $\mu$ s-ms time scale either among multiple ordered states, or between an ordered and disordered state. For tSH2<sub>pm</sub>, many resonances of interdomain A are observed, but the amide and C $\alpha$  and C $\beta$  chemical shifts (data not shown) are near random coil values. There are no trends in the chemical shifts of tSH2<sub>pm</sub> interdomain A consistent with transient helical structure.

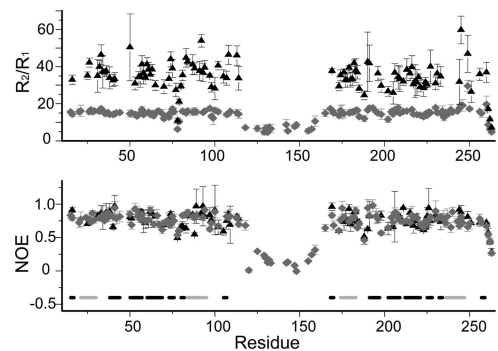


**Fig. 3.** <sup>15</sup>N relaxation data (600 MHz, 293 K) for tSH2 (black) and tSH2<sub>pm</sub> (gray). Heteronuclear NOE values (Lower) and  $R_2/R_1$  values (Upper) are plotted on individual residues basis. The secondary structure elements in the Lower are as follows.  $\beta$ -strand (Black):  $\beta$ A (residues 15–17, 168–171),  $\beta$ B (residues 38–43, 191–196),  $\beta$ C (residues 51–57, 202–209),  $\beta$ D $\beta$ D' (residues 60–69, 212–221),  $\beta$ E (residues 74–76, 225–228),  $\beta$ F (residues 80–82, 232–234),  $\beta$ G (residues 105–107, 257–259).  $\alpha$ -helix (Gray):  $\alpha$ A (residues 22–31, 175–183)  $\alpha$ B (residues 85–93, 237–246). Errors were calculated by pairwise root mean square deviation of duplicate experiments.

Examination of the <sup>15</sup>N HSQC spectrum of a variant Y130F of tSH2 (see SI) finds that the spectra of Y130F tSH2 and wild-type tSH2 are nearly identical. This observation, combined with the similarity of *in vitro* binding to dp-ITAM for Syk(wt) and Syk(Y130F) (Fig. 1A), provides evidence that the tSH2 structure is insensitive to conserved substitution at position 130.

Together, the HSQC chemical shift differences suggest that introduction of negative charge at position 130 induces structural disorder in the linker region, and interactions at the SH2-SH2 interface are altered.

**Changes in Domain Structure Probed by <sup>15</sup>N Relaxation.** The effect of negative charge at position 130 on the overall molecular shape and hydrodynamic behavior of Syk tSH2 was investigated with main-chain amide <sup>15</sup>N relaxation of tSH2 and tSH2<sub>pm</sub> (Fig. 3).

For tSH2, the heteronuclear NOE values (Fig. 3, black) are uniformly close to the slow tumbling limit of 0.83 except for those from residues at the C terminus.  $R_2/R_1$  values vary considerably, consistent with the anisotropic shape of the crystallographic structure of tSH2 (7). The average  $R_2/R_1$  value equals 36.3 and analysis based on rotational anisotropy with crystallographic coordinates for full length tSH2 yielded an overall correlation time of  $\tau_c = 19.2$  ns (Table 1).

Substantially different relaxation behavior is observed for tSH2<sub>pm</sub> (Fig. 3, gray). For residues within the SH2 domains,  $R_2/R_1$  values are  $\approx 15$ , and therefore considerably smaller than those for tSH2.  $R_2$  values are greatly reduced, whereas  $R_1$  values increased relative to tSH2 (see SI). The residue-by-residue variation in  $R_2/R_1$  remains for tSH2<sub>pm</sub> but is less apparent in Fig. 3 because of the reduced range of values expected for smaller  $R_2/R_1$ . Analysis of the relaxation rates finds that both tSH2<sub>pm</sub> and tSH2 tumble anisotropically (see SI). The NOE values from interdomain A resonances are small (average  $\approx 0.2$ ) and reflect internal mobility, which is inferred to be on a faster timescale than the motion of this linker region in tSH2 given that single resonances are observed in tSH2<sub>pm</sub>, whereas these resonances are exchange-broadened in tSH2. Although the slightly positive NOE values for interdomain A in tSH2<sub>pm</sub> are comparable with those for unfolded proteins (21),  $R_2/R_1$  values are significantly larger (5 vs. 2 for unfolded), suggesting conformational mobility intermediate to an ordered tertiary structure and random-coil state. Given the changes in the  $R_2/R_1$  residue profile and the small NOE values of interdomain A, correlation times were estimated for each SH2 domain independently. A value of  $\tau_c \approx 12.2$  ns is estimated for either domain (Table 1).

**Table 1. Comparison of experimental  $R_2/R_1$  (600 MHz, 293 K) and  $\tau_c$  with those predicted from crystal coordinates of Syk tSH2 (PDB entry 1A81), using HYDRONMR(34)**

Protein	Experimental NMR			HYDRONMR prediction*		
	$R_2/R_1$ <sup>†</sup>	Average percent error <sup>‡</sup>	$\tau_c$ , <sup>§</sup> ns	Protein <sup>  </sup>	$R_2/R_1$	$\tau_c$ , ns
tSH2 <sup>  </sup>	36.3	12.3	19.2	tSH2	37.8	19.5
tSH2 <sub>pm</sub> (N-SH2) <sup>  </sup>	15.1	7.8	12.1	N-SH2	6.7	7.6
tSH2 <sub>pm</sub> (C-SH2) <sup>  </sup>	15.8	7.0	12.1	C-SH2	6.5	7.5
tSH2 <sub>pm</sub> (interdomain A) <sup>  </sup>	7.5	27.9	NA	NA	NA	NA

\*Radius of the atomic elements,  $a = 2.5 \text{ \AA}$ , 293 K.

<sup>†</sup>Average taken over residues with  $^1\text{H}-^{15}\text{N}$  NOE > 0.65. Individual residue values for  $R_1$  and  $R_2$  given in supplementary material.

<sup>‡</sup>See SI for definition.

<sup>§</sup>Estimated from the  $R_2/R_1$  values used for the average  $R_2/R_1$ .

<sup>||</sup>tSH2, residues 2–262; N-SH2, residue 9–114; C-SH2, residue 160–262; interdomain A, residue 115–159.

To gain insight into the structural basis for the observed differences in  $R_2/R_1$  values of tSH2 and tSH2<sub>pm</sub>, the experimental results were compared with values predicted from molecular structure by a hydrodynamic analysis, using the program HYDRONMR (Table 1). The values predicted for full-length tSH2, using coordinates for Syk residues 9–262 from the crystallographic structure of the complex with ITAM peptide (PDB 1A81), are  $\tau_c = 19.5$  ns and  $R_2/R_1 = 38$ , which compare well with the respective values of 19.2 ns and 36 from NMR data for the unphosphorylated tSH2. The agreement between the experimental NMR results and the values calculated from molecular structure shows that, in the unphosphorylated state, the SH2 domains are rotationally coupled and suggests the overall molecular shape and orientation of the two domains are similar to those observed crystallographically.

In contrast to tSH2, the relaxation properties of tSH2<sub>pm</sub>, with a negative charge at position 130, indicate faster rotation than full-length tSH2. A perspective on the effective size was sought by comparison with the predicted parameters for isolated SH2 domains (Table 1). For N-SH2 (residues 9–114) and C-SH2 (residues 160–262), the predicted values for  $\tau_c$  are 7.6 ns and 7.5 ns, and the average  $R_2/R_1$  values are 6.7 and 6.5, respectively. The experimentally determined values for  $\tau_c$  (12.1 ns) and the average  $R_2/R_1$  (15.1 and 15.8) for tSH2<sub>pm</sub> are therefore intermediate to the predicted values for full-length tSH2 and isolated SH2 domains. The introduction of negative charge at Y130 therefore acts to partially decouple the SH2 domains by altering the 45-residue interdomain A conformation in a manner that enhances flexibility but retains sufficient compactness to restrain SH2 domain rotation. The decoupling of domain motion in tSH2<sub>pm</sub> infers less contact between the two SH2 domains, and rationalizes the appearance of resonances from the SH2-SH2 interface in tSH2<sub>pm</sub> that are not observed in tSH2 (Fig. 2B).

**Changes in Domain Structure Probed by Residual Dipolar Couplings (RDCs).** Additional information on the decoupling of the two SH2 domains by negative charge at position 130 was obtained from RDCs of mainchain amide groups measured for tSH2 and tSH2<sub>pm</sub>. RDCs, which depend on angular orientation of the N-H bond vector in the molecular alignment frame, were fit for a given domain to a crystallographic model by varying the alignment tensor parameters to minimize differences in observed and calculated RDCs (22). The Euler angles for conversion of the alignment frame to the crystallographic coordinate frame, along with the axial (Aa) and rhombic (R) components of the alignment tensor, were determined by independent optimization of RDCs from either N-SH2 or C-SH2 (Table 2). This procedure of fitting SH2 domains separately provides a more definitive comparison of domain reorientation for tSH2 and tSH2<sub>pm</sub> than a simultaneous fit of the whole structure (see SI).

In the case of tSH2, parameters from independently fitting either N-SH2 or C-SH2 RDCs have similar values (Table 2, rows 2 and 3), and thus the domain orientation in the structural unit for alignment is approximated by the crystal structure shown in Fig. 2B. By contrast, optimal fit of tSH2<sub>pm</sub> RDC data from either N- or C-SH2 yields significantly disparate alignment parameters for Aa and the  $\alpha$  and  $\gamma$  Euler angles (Table 2, rows 4 and 5). Therefore, the domain orientations of tSH2<sub>pm</sub> indicated by alignment are not simultaneously consistent with the crystal structure of Syk tSH2. The RDC data are also not consistent with the SH2 domain orientation in the crystal structure of an unligated form of Zap-70 tSH2, which shows a change in SH2-SH2 orientation of  $\approx 50^\circ$  relative to the complex structure (8) (see SI). Overall, the RDC analysis demonstrates that negative charge at position 130 in tSH2<sub>pm</sub> substantially alters the SH2-SH2 orientation compared with that in unphosphorylated tSH2, although specification of the change in terms of exact structure or domain motion requires further investigation.

**Table 2. Comparison of alignment tensor and sedimentation velocity parameters for tSH2 and tSH2<sub>pm</sub>**

Protein	Domain	$\alpha^*$ , °	$\beta^*$ , °	$\gamma^*$ , °	Aa <sup>†</sup>	R <sup>†</sup>	$R_{\text{dip}}^{\ddagger}$	$n^{\S}$	$s_{20,w}$	$ff/f_0^{\parallel}$
tSH2	N-SH2	80	65	140	-0.00166	0.39	0.37	29	2.61	1.28
	C-SH2	75	82	131	-0.00161	0.59	0.29	26		
tSH2 <sub>pm</sub>	N-SH2	92	49	133	0.00120	0.38	0.34	48	2.28	1.46
	C-SH2	6	31	15	-0.000884	0.44	0.28	50		

Alignment was estimated from RDCs of the N-SH2 and C-SH2 domains independently using the program RDCA (22).

\* $\alpha$ ,  $\beta$ , and  $\gamma$  are Euler angles for the conversion of the alignment tensor frame into the molecular frame.

<sup>†</sup>Aa and R are the unitless axial and rhombic components of the alignment tensor.

<sup>‡</sup> $R_{\text{dip}} = \sqrt{5[(D^{\text{meas}} - D^{\text{calc}})^2]/[2(D^{\text{AB}})^2(4 + 3R^2)]}$ , the quality factor that describes the fit of observed RDCs ( $D^{\text{meas}}$ ) to RDCs calculated from crystal structure ( $D^{\text{calc}}$ ).

<sup>§</sup>Number of RDC values in the fit.

<sup>||</sup>Friction ratio estimated from  $s_{20,w}/s_{\text{ma}}$

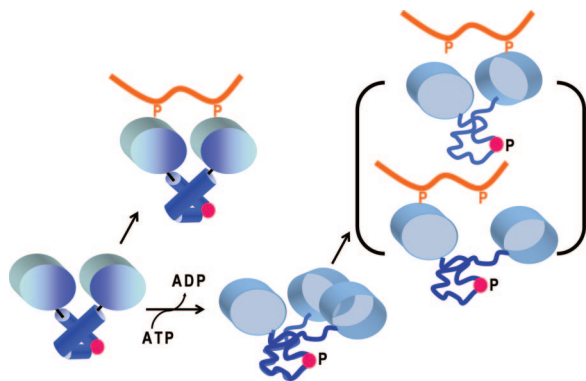


**Fig. 4.** Model of a long-distance mechanism for Y130 (red sphere) phosphorylation to down-regulate association of Syk with the antigen receptor. Phosphorylation destabilizes interdomain A structure, which alters SH2-SH2 domain orientation and retains an increased distance between pY binding sites beyond the limit permitted for bifunctional binding of ITAM.

#### Large-Scale Conformational Change from Sedimentation Velocity.

The large scale conformational difference between tSH2 and tSH2<sub>pm</sub> suggested by <sup>15</sup>N relaxation was further investigated by analytical ultracentrifugation to examine the overall shape of the two proteins. Loosely coupled SH2 domains and a more mobile linker A for tSH2<sub>pm</sub> implies a less compact structure that would exhibit greater viscous drag with correspondingly higher hydrodynamic friction and slower sedimentation by analytical ultracentrifugation than the more compact tSH2. Discretization analysis of sedimentation velocity data (23) yielded an  $s_{20,w}$  value of 2.61 S for tSH2 and 2.28 S for tSH2<sub>pm</sub> with an error of  $\pm 0.05$ S (Table 2). Thus, the expected decrease in  $s_{20,w}$  for tSH2<sub>pm</sub> was observed. The friction ratio,  $ff/f_0$  where  $f$  is the observed frictional coefficient, and  $f_0$  is that of a sphere with equal volume, was correspondingly higher for tSH2<sub>pm</sub> ( $ff/f_0 = 1.46$ ) than for tSH2 ( $ff/f_0 = 1.28$ ). Without interdomain A phosphorylation, tSH2 has a relatively compact domain structure, whereas that of tSH2<sub>pm</sub> is more extended and less spherical in shape.

**Biological Implications.** The role of Y130 phosphorylation in modulating Syk interaction with the B cell receptor proposed earlier (11) is supported here by direct assessment of binding with immobilized dp-ITAM (Fig. 1A) and the 20- to 1,000-fold lower affinity measured for tSH2<sub>pm</sub>. Further, Syk phosphorylated on Y130 can be recovered from anti-IgM-stimulated cells (Fig. 1B), using an epitope tag at the N terminus of Syk to enhance detection from cell lysates. Y130 phosphorylation was demonstrated only in the presence of phosphatase inhibitors (11, 19), likely because of a low phosphorylation level as a result of the dynamics of phosphatase/kinase activity.

We propose a model (Fig. 4) for modulation of Syk receptor binding by Y130 phosphorylation that is a long-distance mechanism based on changes in domain structure. Differences between tSH2 and tSH2<sub>pm</sub> in  $\tau_c$  (Table 1), relative orientation of the two SH2 domains and overall shape (Table 2), and affinity for dp-ITAM indicate that, in tSH2<sub>pm</sub> with negative charge at position 130, the SH2 domains are partly rotationally decoupled but orientationally restricted in a manner that precludes high-affinity ITAM binding. This behavior is in contrast to the tightly coupled SH2 domains of unphosphorylated tSH2, for which the NMR data are modeled relatively well by the crystallographic structure. Negative charge does not simply lead to reorientation of SH2 domains while retaining a joined SH2 structure, as observed crystallographically for unligated Zap-70 tSH2; for tSH2<sub>pm</sub>, the measured RDCs are not fit by the Zap-70 crystal structure and the substantial decrease in  $\tau_c$  suggest the SH2 domains of tSH2<sub>pm</sub> are loosely connected, rather

than only rotated with respect to each other. These results support a model (Fig. 4) in which Syk, without phosphorylation of Y130 in interdomain A, binds receptor with high affinity attributed by two-site binding of the SH2 domains appropriately oriented to fit the separation of two phosphotyrosines in the ITAM. Phosphorylation at position 130 is proposed to destabilize interdomain A conformation, resulting in an altered SH2-SH2 orientation and a more extended structure, less compatible with two-site ITAM binding and with an affinity comparable to single pY binding. By this long-distance mechanism, Y130 phosphorylation of Syk at the membrane would switch Syk from high to low affinity binding of the antigen receptor and release Syk into the cytoplasm. An analogous proposal was made in ref. 24, where conformational destabilization in one domain of a heat-shock protein was found to participate in regulating the function carried out by other domains.

Interdomain A undergoes conformational exchange in solution, suggesting the tertiary structure of this region is marginally stable and disrupted by a perturbation, such as phosphorylation. In the crystal structure of Syk tSH2 bound to peptide (7), Y130 is located in one helix of interdomain A (Fig. 2B). The tyrosyl hydroxyl is neither buried or otherwise sterically confined, nor proximal to acidic residues. As such, this structure does not provide an immediate understanding of the physical basis for the observed structural perturbation from a negative charge at position 130. An analogous effect of tyrosine phosphorylation to negatively regulate molecular association by altering conformational equilibrium was reported for erythrocyte band 3 (25). A region of band 3, recognized by other proteins, forms an ordered loop with Tyr located in the center of the loop. Phosphorylation of this Tyr destabilizes the loop structure and regulates against protein-protein interaction of band 3. The mechanism proposed here for regulation by Y130 phosphorylation similarly inhibits the association of Syk with the receptor by altering conformation of the linker but differs by introducing a destabilizing effect distant to the actual binding site.

Diminished tSH2 binding affinity by SH2-SH2 reorientation can be rationalized in terms of thermodynamic factors. In the crystal structure of the tSH2-peptide complex, ligand interactions span the interface between the two SH2 domains so that optimal binding energy requires proximity of the two domains and altering this interface would diminish binding enthalpy. Two phosphotyrosine binding sites locked in tandem also benefit dp-ITAM binding by an increase in effective local concentration, which enables fast rebinding when one phosphotyrosine dissociates from its binding pocket. The gain from increased effective concentration could be as high as  $10^3$  given the estimated affinities for unphosphorylated and Y130 phosphorylated tSH2. When the two binding sites are not properly positioned, as proposed for the case of phosphorylated tSH2, the individual SH2 domains would recognize only one phosphotyrosine of dp-ITAM with no entropic advantage from two-site binding.

In addition to receptor binding, Y130 phosphorylation is known to alter Syk kinase catalytic activity (11); the intrinsic activity of Syk(Y130E) isolated from unstimulated cells is substantially higher than that of Syk(WT) and the level of Syk(Y130E) activity does not depend on receptor stimulation. Analogous behavior was reported for the Syk variant lacking the tSH2 domain. Thus, similar to activation of Src kinases, regulating Syk in cells under resting conditions appears to depend on the proper organization of the two SH2 domains (26) with the catalytic domain (see below). This organization may be controlled in part by Y130-phosphorylation acting to perturb interdomain A conformation and eliminate an inhibitory effect imposed by specific positioning of the tSH2 relative to kinase domain.

The conclusions of the current work related to Y130 phosphorylation are corroborated by the crystal structure of an autoinhibited form of Zap-70 tyrosine kinase, residues 1–606, and a model for autoinhibition (27). Syk and Zap-70 kinases serve analogous roles in B cells and T cells, respectively, are highly conserved in sequence and tyrosine phosphorylation sites, and the structural mechanisms

for regulating their function are most likely similar. In the assembled structure of autoinhibited Zap-70 (which includes the tandem SH2 region, interdomain B, and the catalytic domain) two helices of interdomain A contact the C-lobe of the catalytic domain on the surface opposite to the catalytic site. The tyrosine residue equivalent to Y130 remains exposed. This interface between interdomain A and the catalytic domain is the basis of the proposed mechanism for autoinhibitory kinase activity (27) in which binding to dp-ITAM is coupled to a conformational change in interdomain A and alters interactions at the interface between interdomain A and the catalytic domain. Destabilization of the interface would promote disassembly of tSH2 from the catalytic domain and facilitate phosphorylation of Zap-70/Syk on tyrosines. Further disruption of SH2-SH2 contact by interdomain A phosphorylation, as described here, would promote kinase release from the membrane if phosphorylation occurs in the disassembled state and would contribute to relief of autoinhibition if phosphorylation occurs in the assembled state. Phosphorylation of interdomain A and B are suggested to be involved with kinase activation (11, 27, 28), whereas only interdomain A phosphorylation is thought to promote antigen-receptor release. It is intriguing to speculate that Y130 phosphorylation redirects the kinase to allow its participation in other signaling pathways as Syk(Y130E) exhibits an enhanced activation of integrins in B cells through “inside-out” signaling (29), and an enhanced association with, and tyrosine-phosphorylation of, centrosomal components in breast cancer cells (30).

## Materials and Methods

**NMR Samples.** Wild-type murine Syk tandem SH2 domain (tSH2), Ser-9-Gln-265, and the tSH2<sub>pm</sub> variant, with Tyr-130 substituted by Glu-130, were <sup>15</sup>N-<sup>13</sup>C-<sup>2</sup>H labeled and purified by affinity chromatography on phosphotyrosine-agarose (see SI for details). Samples were concentrated to 0.7 mM–1 mM in sodium phosphate buffer at pH 7.5 and stored at 4°C. The sample was >95% homogeneous based on SDS/PAGE analysis.

**Phosphopeptide Mapping and Pull-Down Assays.** cDNA for full-length Syk was subcloned into the pCMV-Myc vector (BD Biosciences) to generate a plasmid

coding for Syk with a Myc epitope tag at the N terminus. Syk-deficient DT40 B cells stably expressing Myc-Syk were generated (16). For phosphopeptide mapping experiments, Myc-Syk was immunoprecipitated with an anti-Myc antibody from cells ( $3 \times 10^6$ ) that had been preincubated with 5 mCi [<sup>32</sup>P]orthophosphate and treated for 10 min at 37°C with 10 mM H<sub>2</sub>O<sub>2</sub> or 5 μg/ml goat anti-chicken IgM antibody. The recovered kinase was digested with trypsin and the resulting phosphopeptides were separated by alkaline gel electrophoresis and identified as described in ref. 31. For pull-down assays, lysates from Syk-deficient DT40 cells expressing exogenous Syk, Syk(Y130E), Syk(Y130F), or catalytically inactive Syk(K396R) (KD) that had been treated with or without 10 mM H<sub>2</sub>O<sub>2</sub> were applied to a biotinylated dp-ITAM peptide immobilized on streptavidin-agarose. Adsorbed proteins were separated by SDS/PAGE and analyzed by Western blot with an anti-Syk antibody. The relative levels of binding were determined by densitometry.

**<sup>15</sup>N Relaxation and Residual Dipolar Couplings (RDC).** Mainchain resonances assignments for tSH2 and tSH2<sub>pm</sub> identified 96% of the HSQC peaks. <sup>15</sup>N relaxation rates were measured at 600 MHz field strength, 293 K, in duplicate and  $R_1$ ,  $R_2$ , and NOE values extracted for 97 residues of Syk tSH2 and 134 residues of tSH2<sub>pm</sub>. Correlation times and anisotropic tensors were determined from  $R_1$ ,  $R_2$ , and crystallographic coordinates, using the program TENSOR2.0. Alignment parameters were estimated from N-H RDCs obtained in the presence of filamentous phage Pf1, using the MATLAB-based program RDCA (22) and an input molecular structure.

**Analytical Ultracentrifugation.** Protein samples were sedimented at 50,000 rpm for 8 h. Experimental  $s$  values from SEDFIT (32) were corrected to obtain  $s_{20,w}$ . The degree of asymmetry was estimated from  $s/s_{max}$  values by SEDNTERP (www.jphilo.mailway.com).

Equilibrium binding constants for dp-ITAM associating with different Syk constructs were determined by using a final peptide concentration ranging from 1 μM to 10 μM. The concentration of 5'-carboxyfluorescein-dp-ITAM peptide was determined from 490-nm absorbance and the concentration of protein from Rayleigh interference fringe displacement.  $K_D$  was estimated from five sets of binding data, using Origin software. Details are in SI.

**ACKNOWLEDGMENTS.** We thank Drs. Nikolai Skrynnikov and David Goldenberg for valuable discussions. This work was supported by National Institutes of Health Grant GM39478 (to C.B.P.), a Purdue University reinvestment grant, and Purdue Cancer Center Grant CA23568.

- Turner M, Schweighoffer E, Colucci F, Di Santo JP, Tybulewicz VL (2000) Tyrosine kinase SYK: Essential functions for immunoreceptor signalling. *Immunol Today* 21:148–154.
- Reth M (1989) Antigen receptor tail clue. *Nature* 338:383–384.
- Koyasu S, et al. (1994) Delineation of a T-cell activation motif required for binding of protein tyrosine kinases containing tandem SH2 domains. *Proc Natl Acad Sci USA* 91:6693–6697.
- Gruza RA, Futterer K, Chan AC, Waksman G (1999) Thermodynamic study of the binding of the tandem-SH2 domain of the Syk kinase to a dually phosphorylated ITAM peptide: Evidence for two conformers. *Biochemistry* 38:5024–5033.
- Ottinger EA, Botfield MC, Shoelson SE (1998) Tandem SH2 domains confer high specificity in tyrosine kinase signaling. *J Biol Chem* 273:729–735.
- Kumaran S, Gruza RA, Waksman G (2003) The tandem Src homology 2 domain of the Syk kinase: A molecular device that adapts to interphosphotyrosine distances. *Proc Natl Acad Sci USA* 100:14828–14833.
- Futterer K, Wong J, Gruza RA, Chan AC, Waksman G (1998) Structural basis for Syk tyrosine kinase ubiquity in signal transduction pathways revealed by the crystal structure of its regulatory SH2 domains bound to a dually phosphorylated ITAM peptide. *J Mol Biol* 281:523–537.
- Folmer RH, Geschwindner S, Xue Y (2002) Crystal structure and NMR studies of the apo SH2 domains of ZAP-70: Two bikes rather than a tandem. *Biochemistry* 41:14176–14184.
- Rolli V, et al. (2002) Amplification of B cell antigen receptor signaling by a Syk/ITAM positive feedback loop. *Mol Cell* 10:1057–1069.
- Neumeister EN, et al. (1995) Binding of ZAP-70 to phosphorylated T-cell receptor zeta and eta enhances its autophosphorylation and generates specific binding sites for SH2 domain-containing proteins. *Mol Cell Biol* 15:3171–3178.
- Keshvara LM, Isaacson C, Harrison ML, Geahlen RL (1997) Syk activation and dissociation from the B-cell antigen receptor is mediated by phosphorylation of tyrosine 130. *J Biol Chem* 272:10377–10381.
- Groesch TD, Zhou F, Mattila S, Geahlen RL, Post CB (2006) Structural basis for the requirement of two phosphotyrosine residues in signaling mediated by Syk tyrosine kinase. *J Mol Biol* 356:1222–1236.
- Deckert M, Tartare-Deckert S, Couture C, Mustelin T, Altman A (1996) Functional and physical interactions of Syk family kinases with the Vav proto-oncogene product. *Immunity* 5:591–604.
- Hong JJ, Yanke TM, Harrison ML, Geahlen RL (2002) Regulation of signaling in B cells through the phosphorylation of Syk on linker region tyrosines. A mechanism for negative signaling by the Lyn tyrosine kinase. *J Biol Chem* 277:31703–31714.
- Peters JD, Furlong MT, Asai DJ, Harrison ML, Geahlen RL (1996) Syk, activated by cross-linking the B-cell antigen receptor, localizes to the cytosol where it interacts with and phosphorylates alpha-tubulin on tyrosine. *J Biol Chem* 271:4755–4762.
- Zhou F, Hu J, Ma H, Harrison ML, Geahlen RL (2006) Nucleocytoplasmic trafficking of the Syk protein tyrosine kinase. *Mol Cell Biol* 26:3478–3491.
- Sloan-Lancaster J, et al. (1997) Regulation of ZAP-70 intracellular localization: Visualization with the green fluorescent protein. *J Exp Med* 186:1713–1724.
- Furlong MT, et al. (1997) Identification of the major sites of autophosphorylation of the murine protein-tyrosine kinase Syk. *Biochimica et biophysica acta* 1355:177–190.
- Yanke TM, Keshvara LM, Sawasdikosol S, Harrison ML, Geahlen RL (1999) Inhibition of signaling through the B cell antigen receptor by the protooncogene product, c-Cbl, requires Syk tyrosine 317 and the c-Cbl phosphotyrosine-binding domain. *J Immunol* 163:5827–5835.
- Chen T, et al. (1996) Interaction of phosphorylated FcεpsilonRIγ immunoglobulin receptor tyrosine activation motif-based peptides with dual and single SH2 domains of p72syk. Assessment of binding parameters and real time binding kinetics. *J Biol Chem* 271:25308–25315.
- Wirmer J, Peti W, Schwalbe H (2006) Motional properties of unfolded ubiquitin: A model for a random coil protein. *J Biomol Nmr* 35:175–186.
- Skrynnikov NR, et al. (2000) Orienting domains in proteins using dipolar couplings measured by liquid-state NMR: differences in solution and crystal forms of maltodextrin binding protein loaded with beta-cyclodextrin. *J Mol Biol* 295:1265–1273.
- Lebowitz J, Lewis MS, Schuck P (2002) Modern analytical ultracentrifugation in protein science: A tutorial review. *Protein Sci* 11:2067–2079.
- Ilbert M, et al. (2007) The redox-switch domain of Hsp33 functions as dual stress sensor. *Nat Struct Mol Biol* 14:556–563.
- Schneider ML, Post CB (1995) Solution structure of a band 3 peptide inhibitor bound to aldolase: A proposed mechanism for regulating binding by tyrosine phosphorylation. *Biochemistry* 34:16574–16584.
- Hatada MH, et al. (1995) Molecular basis for interaction of the protein tyrosine kinase ZAP-70 with the T-cell receptor. *Nature* 377:32–38.
- Deindl S, et al. (2007) Structural basis for the inhibition of tyrosine kinase activity of ZAP-70. *Cell* 129:735–746.
- Zhao Q, Williams BL, Abraham RT, Weiss A (1999) Interdomain B in ZAP-70 regulates but is not required for ZAP-70 signaling function in lymphocytes. *Mol Cell Biol* 19:948–956.
- Stupack DG, et al. (1999) Matrix valency regulates integrin-mediated lymphoid adhesion via Syk kinase. *J Cell Biol* 144:777–788.
- Zyss D, et al. (2005) The Syk tyrosine kinase localizes to the centrosomes and negatively affects mitotic progression. *Cancer Res* 65:10872–10880.
- Keshvara LM (1998) In *Medicinal Chemistry and Molecular Pharmacology* (Purdue Univ Press, West Lafayette, IN).
- Schuck P (2000) Size-distribution analysis of macromolecules by sedimentation velocity ultracentrifugation and lamm equation modeling. *Biophys J* 78:1606–1619.
- Ayed A, et al. (2001) Latent and active p53 are identical in conformation. *Nat Struct Biol* 8:756–760.
- García de la Torre J, Huertas ML, Carrasco B (2000) HYDRONMR: Prediction of NMR relaxation of globular proteins from atomic-level structures and hydrodynamic calculations. *J Magn Reson* 147:138–146.